

Preliminary Studies of Various Rotor Pole Number for Permanent Magnet Flux Switching Machines (PMFSM)

Laili Iwani Jusoh, Erwan Sulaiman, Rajesh Kumar, Fatimah Shafiqah Bahrim & M. Fairoz Omar

*Department of Electrical Power Engineering, Universiti Tun Hussein Onn Malaysia
Line 3- Locked Bag 101, Batu Pahat, Johor, 86400 Malaysia.*

Abstract

In this paper, a study on the slot and pole number combinations of the single-phase permanent magnet flux-switching machine (PMFSM) has been executed. Four slot designs namely 2S-8P, 4S-8P, 8S-12P, and 10S-15P were chosen by analysing the highest power value and torque in the rotor pole study. The proposed designs were briefly compared in regards to topology development, material and conditions setting as well as properties setting. A few analyses have been carried out such as cogging torque, output power and torque, and speed. This study was carried out using JMAG Designer version 14.0 with 2D finite-element analysis (2D-FEA). The simulated result showed that the proposed design 4S-8P was the best with produce higher torque with 2.47Nm significantly 33% better than the 8S-12P and 10S-15P which come in second place with 1.65Nm and 1.7Nm respectively.

Keywords: permanent magnet flux switching machine, single phase.

INTRODUCTION

This In the middle of 1950s, the concept of the FSM was founded and first published [10]. Several novel and new FSM machine topologies have been established for various applications, ranging from low cost domestic appliances, automotive, wind power, to aerospace and getting more popular in recent years.

The new flux-switching motor is a very simple motor to manufacture, and coupled with a power electronic controller demanding only two power semiconductor switches, it has the potential to be low cost in high volume applications. Furthermore, flux switching machine has an electronically commutated brushless motor, essentially offers longer life and very flexible and precise control of torque, speed, and position at no additional cost [1]. FSM has been seen as a potential candidate for future variable speed applications because of its unique merits [2].

Ordinarily, the FSMs can be characterised into three cluster that are field excitation flux switching machine (FEFSM), permanent magnet flux switching machine (PMFSM), and hybrid excitation flux switching machine (HEFSM) [6]. Both PMFSM and FEFSM have only one primary source of excitation flux, respectively induced by the permanent magnet and the field excitation coil whereas both PM and FECs both are used for generating flow in HEFSM [7].

Based on the literature review, analysis of the number combinations of slots and poles of machine designs should be made in enhancing a machine's performance [3]. Various combination of stator slot and rotor pole for HEFSM have been refined for high speed applications [4]. An early example of FEFSM also has been proposed by the author. The impact of rotor pole number on the characteristics of single-phase has been presented. Four topologies 12S-3P, 12S-6P, 12S-9P and 12S-15P of single phase FEFSM with the segmental rotor and non-overlap windings have been investigated and compared [6].

In other proposed example is study of rotor pole number for ORHEFSM. This paper show the rotor pole number effect on the characteristics of outer-rotor hybrid excitation flux switching motor (ORHEFSM) for in-wheel drive electric vehicle (EV) applications. The appropriate number of slot pole play a key role in order to define the optimal performances [9]. The permanent magnet flux switching machine (PMFSM) has been a popular research topic because of its high power density and robust rotor structure . With both PMs and armature windings located in the stator and single solid piece rotor similar to the switched reluctance machine, PMFSM has the advantage of suitability for high speed drives and easy cooling of all active parts compared to conventional PM machines PM [5].

Based on the literature review, design a new structure of 12S-10P PMFSM has been proposed by the researcher for Hybrid Electric Vehicle (HEV) applications, the results and working principle and working principle has also been discussed [5]. Even so, this paper initially presents the comparative combinations of single phase PMFSM number slots and poles of proposed motor designs namely 2S-8P, 4S-8P, 8S-12P, and 10S-15P. In this study, the possible number of rotor pole and stator slot is defined by (1).

$$N_r = N_s \left(1 \pm \frac{k}{2q} \right) \quad (1)$$

Where N_r is the number of rotor poles, N_s is the number of stator slots, k is the natural entity having value 1,2,3 and q is the number of phases. Whereas, the electrical frequency, f_e of the proposed motors can be expressed by (2).

$$f_e = N_r \cdot f_m \quad (2)$$

Where f_e is the electrical frequency, f_m is the mechanical rotation frequency and N_r is the number of rotor poles respectively. The armature coil current and number of turns are calculated using (3) and (4), respectively. The motor's filling factor is set at 0.5, to ensure flux moves from the stator to rotor

equally without any flux leakage, the design of the proposed machines is defined as in (5).

$$I_a = \frac{J_a \alpha S_a}{N_a} \quad (3)$$

$$N_a = \frac{\alpha S_a}{A_{copper}} \quad (4)$$

$$\sum \text{Stator Tooth Width} = \sum \text{Rotor Tooth Width} \quad (5)$$

Where N, J, α , S, A and I are number of turns, current density, filling factor, slot area, copper width and input current, respectively. The subscript a is represent for armature coil. Initially, the rotor, stator and armature coil of the proposed design are drawn by using Geometry Editor by JMAG-Designer ver. 14.0, released by the Japan Research Institute (JRI).

The effects of slot pole number combinations on the electromagnetic performance such as cogging torque, flux linkage, back electromagnetic force (back-emf), output torque, and power were analyzed based on 2-D finite element analysis (FEA). Table 1 shows the rotor pole study for each slot number.

TABLE I. PERFORMANCE OF DESIGN ROTOR POLE STUDY

Ns	Nr	Flux Linkage ϕ	Back Emf	Cogging Torque (Nm)	Torque (Nm)	Power (W)
2	4	0.3	54.6	1.76	0.816	34.34
	6	0.29	66.94	1.96	1.37	53.94
	8	0.26	121.01	0.58	1.45	56.50
4	6	0.04	15.09	0.47	2.21	131.40
	8	0.21	94.32	3.85	2.47	212.20
	10	0.03	23.49	0.66	1.97	111.00
	12	0.102	44.80	6.03	1.43	75.00
8	4	0.01	2.84	0.72	0.25	93.13
	12	0.06	5.20	1.12	1.65	312.30
	16	0.02	13.20	15.8	0.88	138.80
	20	0.02	3.34	0.67	0.52	104.30
	24	0.02	19.50	4.27	1.07	168.80
10	15	1.88	18.40	3.99	1.71	402.7
	20	1.81	14.52	18.72	1.43	34.72
	25	6.80	8.46	3.26	0.96	27.45

VARIOUS DESIGN TOPOLOGIES AND SPECIFICATION

PMFSM with wound salient rotor structure is illustrated in Fig. 1. The proposed topology is clearly seen to have four design which is 2slot-8pole, 4slot-8pole, 8slot-12pole and 10slot-15pole. These designs were considered as the best pole combination in rotor pole study as it resulting in high average torque and high power.

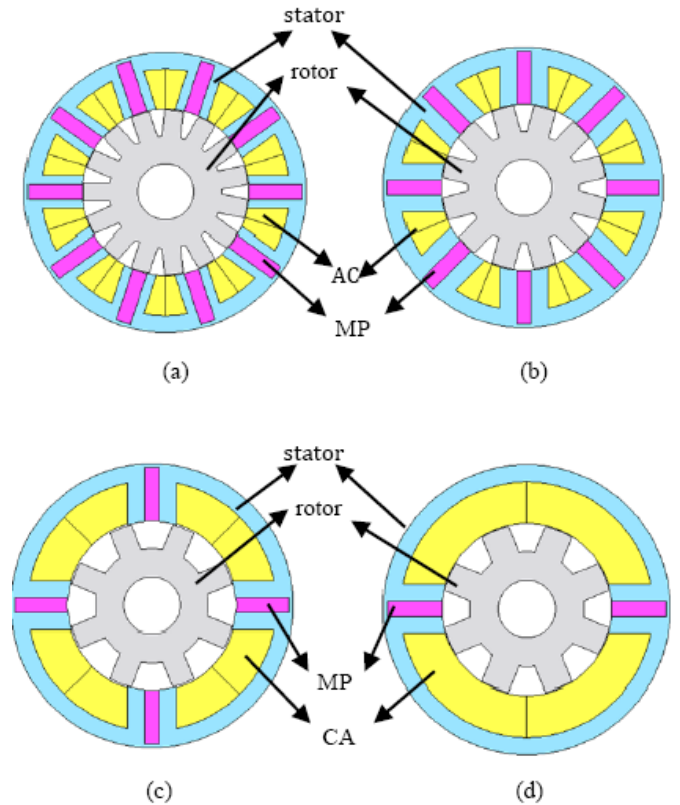


Figure 1. Slot pole study a) 10S-15P, b) 8S-12P, c)4S-8P, d) 2S-8P

Similarly, all the armature phases employ the similar winding configurations and embedded in the stator core to form the winding slot. In addition, PMs with the arrangement of alternate circumferential directions at every rotor tooth are employed.

Since PM volume is limited to only 70g, the final machine is more likely to have less weight but in contrast much high performances to be obtained in terms of output torque and power. The type of PM material used in developing the design is Neomax35AH, while for rotor and stator parts are made up of electrical steel coded 35A250. The design restrictions and parameters of the proposed design are presented in Table 2.

TABLE II. DESIGN RESTRICTION AND SPECIFICATION OF FSM MACHINE

Items	2S-8P	4S-8P	8S-12P	10S-15P
No. of phase			1	
Stator inner radius(mm)			22.25	
Stator outer radius(mm)			37.5	
Rotor outer radius(mm)			22	
Rotor inner radius(mm)			7.5	
Rotor tooth width(mm)	7.5	6	6	5

Stator tooth width(mm)	9	9	9	5
Motor stack length(mm)	20.3			
Air gap length (mm)	0.25			
PM Volume (g)	70			

RESULT AND PERFORMANCE BASED ON 2D-FINITE ELEMENT ANALYSIS

A. Flux lines and Flux Distribution

- The flux lines and flux distribution for the initial design of the single phase are prove in Fig.2 and Fig.3 respectively. From Fig. 2, the proposed design of 2S-8P, 4S-8P, 8S-12P and 10S-15P show that flux lines move from the stator and return through to the nearest rotor pole to make a complete flux cycle.

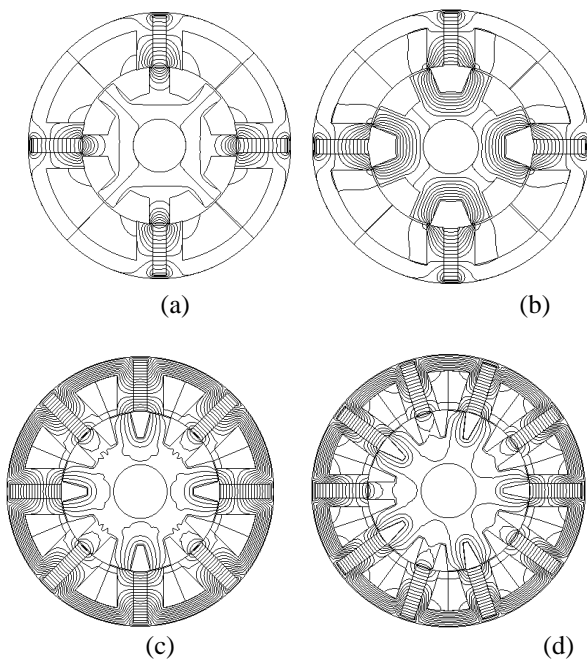


Figure 2. Flux lines of FSM a) 2S-8P, b) 4S-8P, c) 8S-12P, d) 10S-15P

- The flux path for PMFSM is generated at the PM and armature coil. Furthermore, the flux distribution is investigated to monitor field saturation effect on the machine as shown in Fig.3 (a), Fig. 3(b), Fig. 3(c) and Fig. 3(d). Evidently, all the design machines have surfaced almost identically excited PM flux lines and distributions similarity as the flux surges from stator to rotor and return through the rotor teeth to generate in a complete flux cycles of PM.

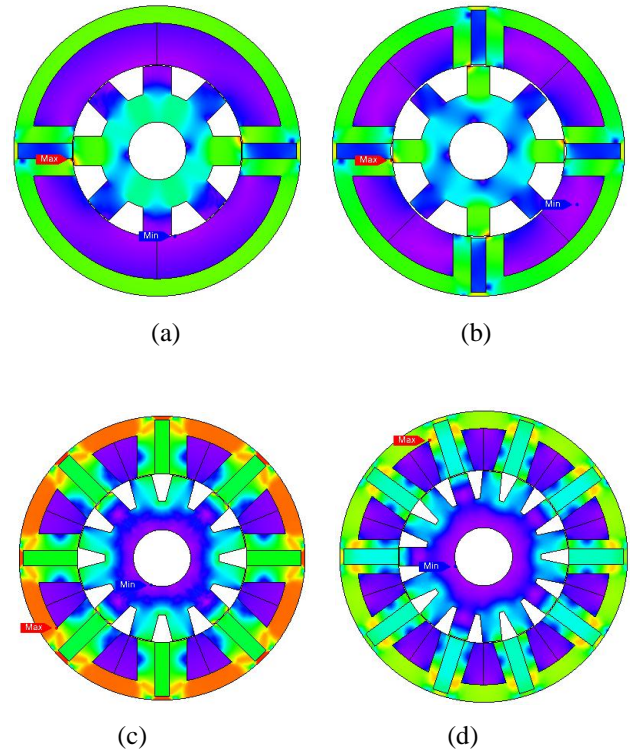


Figure 3. Flux distribution of FSM a) 2S-8P, b) 4S-8P, c) 8S-12P, d) 10S-15P

B. Cogging Torque

The cogging torque analyses for all machine types were diagnosed by setting armature current density, $J_a=0$ Arms/mm². Figure 4 shows the cogging torque investigation of the examined PMFSM design machines, with 4S-8P having the highest peak-to-peak cogging torque at approximately 3.85Nm, followed by 10S-15P, 8S-12P, and 2S-8P at 3.99Nm, 1.12Nm, and 0.58Nm, respectively. The high cogging torque can be relatively reduced as the study continued at the stage of design refinement and optimization. Based on the previous study, cogging torque could be further decrease by rotor pole-notching, rotor pole-pairing and rotor skewing.

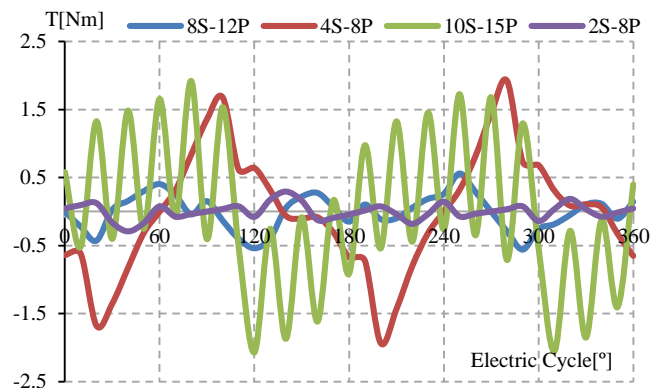


Figure 4. Cogging torque performance for 10S-15P, 8S-12P, 4S-8P and 2S-8P

C. Initial Torque Performances

- The resulting data of initial torque performances for four design machines are plotted in Fig.5. The investigation of torque performances was carried out at maximum armature current densities, $J_a=30$ Arms/mm² for all design machines. Figure 5 shows performances of output torque for all PMFSM designs, and 4S-8P computed the highest performance at 2.47Nm, followed by 2S-8P, 8S-12P, and 10S-15P at 1.45Nm, 1.65Nm, and 1.70Nm, respectively.

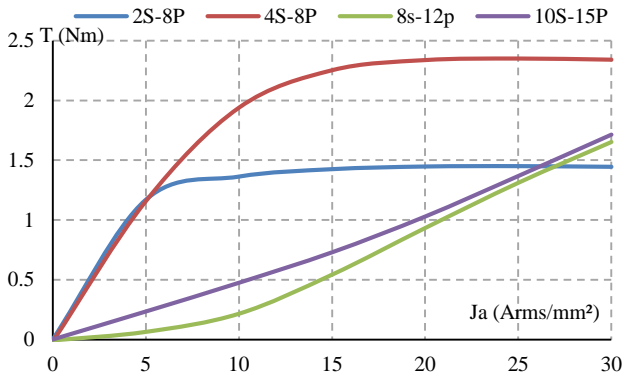


Figure 5. Output torque versus armature current densities, J_a

- The calculation of output power can be executed by manipulating the data of torque and speed. Since all the required data have been obtained in the previous analysis, equation (8) is used to substitute them in. Subsequently, for the rotational on a fixed axis, the calculated power is equal to the multiplication between torque and angular velocity of the rotating piece, which are defined by equations (6), (7), and (8).

$$P = \tau\omega \tag{6}$$

$$\omega = \frac{2\pi S}{60} \tag{7}$$

$$P = \tau \left(\frac{2\pi S}{60} \right) \tag{8}$$

- Where P is power in kilowatt (kW), τ is torque in Newton metre (Nm), and S is speed in revolution per minute (r/min). Therefore, Fig. 6 emphasizes on the 10S-15P design, which has contributed to the highest output power, approximately 402.7W, followed by 8S-12P, 4S-8P, and 2S-8P at 312.38W, 212.2W, and 56.5W, respectively.

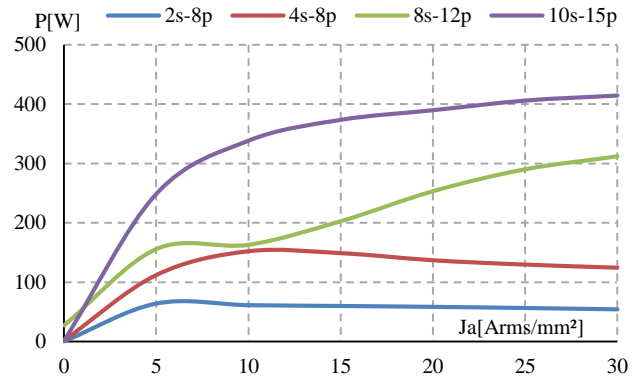


Figure 6. Output power versus armature current densities, J_a

D. Torque and Power Versus Speed

- The torque and power versus speed curves of the designed PMFSM design of, 10S-15P, 8S-12P, 4S-8P and 2S-8P is plotted in Fig. 7, and Fig. 8. The analysis results shows that design torque versus speed of 10S-15P, the initial speed 2327 r/min and the resulting torque is 1.65Nm, while the corresponding power reaches 402.7W. Design slot 8S-12P at the initial speed of 1805 r/min, the resulting torque is 1.65Nm, less compared to 10S-15P FEFSM with corresponding power reaches 312.38W.
- Design slot 4S-8P with the initial speed of 821.55 r/min, the resulting torque is 2.47Nm and power with 212.2W. Finally, for the design 2S-8P shows the initial speed of 371.54Nm, torque at 1.45Nm, with corresponding power reaches 56.5W. As a final point, the overall performances of the proposed machine designs are visualized in Table 3. The resulting data of initial torque performances for four design machines are plotted in Fig.5. The investigation of torque performances was carried out at maximum armature current densities, $J_a=30$ Arms/mm² for all design machines. Figure 5 shows performances of output torque for all PMFSM designs, and 4S-8P computed the highest performance at 2.47Nm, followed by 2S-8P, 8S-12P, and 10S-15P at 1.45Nm, 1.65Nm, and 1.70Nm, respectively.

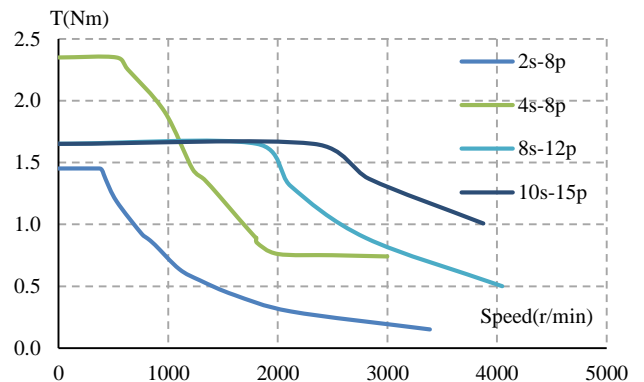


Figure 7. Torque versus speed characteristic 10S-15P PMFSM

TABLE III. PERFORMANCES COMPARISON OF SLOT NUMBER AND POLE

Number of Slot Pole	Cogging torque (Nm)	Maximum power (W)	Maximum torque (Nm)	Speed (r/min)
2S-8P	0.58	56.50	1.45	371.54
4S-8P	3.85	212.20	2.47	821.55
8S-12P	1.12	312.40	1.65	1805.40
10S-15P	3.00	402.7	1.65	2327.4

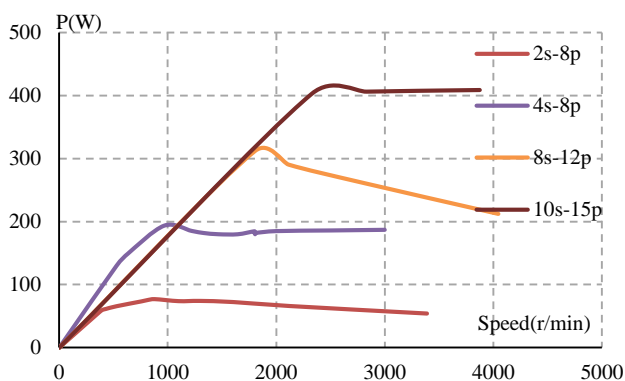


Figure 8. Power versus speed characteristic 8S-12P PMFSM

E. Instantaneous Torque Characteristics

The instantaneous torque profile for initial 2S-8P, 4S-8P, 8S-12P and 10S-15P is illustrated in Fig. 9. The 4S-8P design has the higher torque which is approximately 2.30Nm more than 10S-15P, 8S-12P and 2S-8P design which is torque is at 1.72Nm, 1.64Nm and 1.44Nm respectively. Meanwhile, the peak-peak torque for 4S-8P design is highest at 3.85Nm. Although peak-peak of the instantaneous torque for 4S-8P is high, further design refinement and improvement will be conducted in the future to get the target torque, as well as a method of reducing the cogging torque. Resulting data of initial torque performances for four design machines are sketched in Fig. 5. The investigation of torque performances was carried out at maximum armature current densities, $J_a=30$ Arms/mm² for all design machines. Figure 5 shows performances of output torque for all PMFSM designs, and 4S-8P computed the highest performance at 2.47Nm, followed by 2S-8P, 8S-12P, and 10S-15P at 1.45Nm, 1.65Nm, and 1.70Nm, respectively.

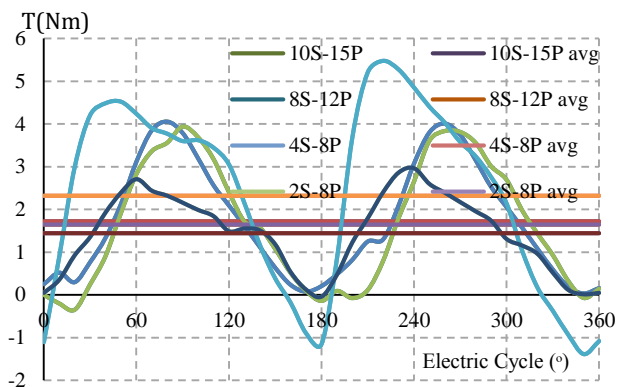


Figure 9. Instantaneous torque of 10S-15P, 8S-12P, 4S-8P and 2S-8P PMFSM

CONCLUSION

In this paper, the analysis of the slot pole combination for the single-phase PMFSM has been carried out and compared. The initial output performances for flux distribution, cogging torque, speed, output power, and torque have been examined. As a result, the 4S-8P PMFSM structure has composed the highest initial output torque, which produced 2.47Nm, compared with the other three designs namely 2S-8P at 1.45Nm, 8S-12P, and 10S-15P at 1.65Nm and 1.71Nm respectively.

ACKNOWLEDGMENT

This research was partly sponsored by the Centre for Graduate Studies UTHM and Ministry of Higher Education Malaysia (MOHE).

REFERENCES

- [1] A. Z. Husin, E. Sulaiman, and T. Kosaka, "Design studies and effect of various rotor pole number of field excitation flux switching motor for hybrid electric vehicle applications," IEEE 8th International Power Engineering and Optimization Conference (PEOCO), IEEE 8th International, Langkawi, pp. 144-149, 2014
- [2] C. Pollock, H. Pollock, R. Barron, J. R. Coles, D. Moule, A. Court and R. Sutton, "Flux-switching motors for automotive applications," IEEE Transactions on Industry Applications, vol. 42, no. 5, pp. 1177-1184, October 2006
- [3] E. Hoang, M. Lecrivain and M. Gabsi, "A new structure of a switching flux synchronous polyphased machine with hybrid excitation," Power Electronics and Applications Conference, European Aalborg, pp. 1-8, 2007
- [4] E. Sulaiman, M. Z. Ahmad, T. Kosaka, and N. Matsui, "Design optimization studies on high torque and high power density hybrid excitation flux switching motor for HEV," Procedia Engineering, Vol. 53, pp. 312-322, March 2013.

- [5] E. Sulaiman, T. Kosaka, Y. Tsujimori and N. Matsui, "Design of 12-slot 10-pole permanent magnet flux-switching machine with hybrid excitation for hybrid electric vehicle," *Power Electronics, Machines and Drives (PEMD)*, 5th IET International Conference on, Brighton, UK, pp. 1-5, 2010
- [6] M. F. Omar, E. Sulaiman, F. Khan, G. M. Romalan and M. K. Hassan, "Performances comparison of various design slot pole of Field Excitation Flux Switching Machines with segmental rotor," *IEEE Conference on Energy Conversion (CENCON)*, Johor Bahru, pp. 320-324, 2015
- [7] M. Jenal and E. Sulaiman, "Investigative study of a novel permanent magnet flux switching machine employing alternate circumferential and radial permanent magnet," *ARPN Journal of Engineering and Applied Sciences*, Vol. 10, pp. 6513-6519, 2015
- [8] M. Z. Ahmad, E. Sulaiman, Z. A. Haron, and F.Khan, "FEA-Based design study of 12-slot 12-pole outer-rotor dual excitation flux switching machine for direct drive electric vehicle applications," *Applied Mechanics and Materials*, Vol. 660, pp. 836-840, August 2014
- [9] M. Z. Ahmad, E. Sulaiman, Z. A. Haron and Kosaka, "Impact of rotor pole number on the characteristics of outer rotor hybrid excitation flux switching motor for in wheel drive EV," *International Conference on Electrical Engineering and Informatics (ICEEI)*, pp. 593-601, 2013
- [10] S. E. Rauch and L. J. Johnson, "Design principles of flux-switch alternators," *Transactions of the American Institute of Electrical Engineers. Part III: Power Apparatus and Systems*, vol. 74, January 1955